IEEE Access
Multidisciplinary | Rapid Review | Open Access Journal

Received April 10, 2022, accepted April 28, 2022, date of publication May 9, 2022, date of current version May 17, 2022.

Digital Object Identifier 10.1109/ACCESS.2022.3173605

Delay-Dependent Sliding Mode Variable Structure Control of Vehicle Magneto-Rheological Semi-Active Suspension

MAOFEI ZHU[1,2], GANG LV[1], CHUNPENG ZHANG[1], JIANMAN JIANG[3], AND HUIRAN WANG[1]

[1]School of Advanced Manufacturing Engineering, Hefei University, Hefei 230601, China
[2]Anhui Provincial Engineering Technology Research Center of Intelligent Vehicle Control and Integrated Design Technology, Hefei 230601, China
[3]Technical Center, Anhui Jianghuai Automobile Company Ltd., Hefei 230601, China

Corresponding author: Chunpeng Zhang (zhangchunpeng@hfuu.edu.cn)

This work was supported in part by the University Natural Sciences Research Project of Anhui Province under Grant KJ2021A0988, in part by the Talent Research Fund Project of Hefei University under Grant 20RC06, and in part by the Anhui Provincial Development and Reform Commission 2020 New Energy Vehicle Industry Innovation Development Project under Grant wfgcyh2020477.

ABSTRACT The vehicle semi-active suspension with Magneto-Rheological Damper (MRD) has been a hot research topic of this decade, featuring the challenging task of the robust control with actuator time delay considerations. In this study, a delay dependent sliding mode variable structure control, based on the Linear Matrix Inequality (LMI), is proposed to suppress the vibration of the Magneto-Rheological Semi-Active Suspension (MRSS) control system. In accordance with the nonlinear characteristics of MRD, a dynamic model of automotive semi-active suspension system, considering time delay, is established. By defining a parameter-dependent Lyapunov switching functional, the conditions for asymptotic stability of closed-loop time delay system are derived, while the sliding mode variable structure control with reduced conservatism is designed. According to the method of LMI, the asymptotic stability problem of sliding mode is transformed into a feasibility problem, which can be solved by the solver 'feasp' in LMI toolbox. In addition, the calculation of the critical time delay of MRSS is expressed as a generalized eigenvalue optimization problem. For comparison purposes, three representative controllers, including a conventional sliding mode controller, a delay dependent controller, and a smith compensation, are studied. Simulation and real vehicle testing on bump and random road responses show that, the designed delay dependent controller can ensure the stability of the suspension system, weaken the influence of time delay on the control performance and effectively improve the ride comfort of the vehicle.

INDEX TERMS Semi-active suspension, magneto-rheological damper, time delay, sliding mode variable structure control, linear matrix inequality.

I. INTRODUCTION

The design of an efficient vehicle suspension control system is an important task, attracting considerable attention, since it can significantly improve passenger comfort, safety and vehicle maneuverability. From the perspective of the control design, the vehicle suspension system can be classified as passive, active and semi-active suspension [1], [2]. Attenuating the harmful effects of the vibrations, due to various road conditions, is the primary objective of any suspension system. Due to their nature, passive suspension systems are faced with an inherent trade-off between the ride quality and handling performance, whereas the application of active suspension systems is limited by their large power consumption and expensive hardware. In the past decade, semi-active suspension systems have received considerable attention, since they can provide a superior performance to that of passive suspensions, without incurring the cost and complexity associated with fully active systems [3].

At present, the research of semi-active suspension mainly focuses on adjusting the damping coefficient of the shock absorber. The adjustment of the damping coefficient of a shock absorber includes stage and stepless adjustment. By opening and closing the control valve, a stage adjustable shock absorber can quickly switch the damping effect

The associate editor coordinating the review of this manuscript and approving it for publication was Zheng Chen.

This work is licensed under a Creative Commons Attribution 4.0 License. For more information, see https://creativecommons.org/licenses/by/4.0/

between several discrete values [4], [5]. The structure and control system of the stage adjustable shock absorber are relatively simple, but there are some limitations regarding the ability of adapting to varying driving conditions and road conditions. The damping coefficient of stepless adjustable damper can continuously change within a certain range, meaning throttling aperture adjustment and magneto-rheological fluid viscosity adjustment [6]. Magneto-Rheological Dampers(MRDs) can change their damping characteristics in response to changes in the strength of a magnetic field generated by embedded electromagnets. Thus, MRDs have no moving parts, making for a simpler, cheaper and more durable structure [7]–[11].

However, one challenge in the use of MRD is the development of a robust control algorithm for the suspension system. Several control strategies have been proposed for semi-active suspension. These control strategies include semi-active control algorithms [12], linear feedback control algorithms [13] and modern intelligent control strategies [14]–[16]. The above studies have significantly improved the performance of the Magneto-Rheological Semi-Active Suspension (MRSS) system but lack consideration for the time delay in actuator dynamics. There is inevitable time delay in the control procedure, which arises from measuring system variables, determining and computing the control laws and finally implementing the control force application. Although the time delay may be short, it can limit the control performance, when the delay appears in the feedback loop [17], [18]. Hu and Wang [19] studied in detail the nonlinear dynamics in vibration control systems with time delay, deriving some important criteria for stability analysis of systems with delayed feedback. Hosek *et al.* [20] applied delayed MRD to the vibration control in rotating mechanical structures, due to multi degree of freedom tensional oscillations and discussed the stability condition deduced from time delay. Jalili and Olgac [21] extended the above results to a MRSS, using partial state feedback with controlled time delay, while the parameters range for stable motion and the sensitivity analysis were also discussed. According to these studies of the influence of time delay on control systems, unsuitable time delay will affect the stability of the controlled system and inevitably deteriorate the performance of the MRSS.

In order to overcome the actuator time delay problem, one approach is to design a compensator, acting in parallel with the controlled object, to weaken and eliminate the influence of time delay on the control performance. In [22] a smith predictor was designed to compensate the input time delay, so that the closed-loop system became a delay-free system. Zhou [23] studied the input delay compensation of control systems with input delay and designed a nested-pseudo compensator, to predict the future states, so that the input delay, which can be arbitrarily large yet bounded, is completely compensated. Furthermore, Taylor series expansion is a frequently used compensation method, where time delay is compensated by expanding the state vectors into Taylor series and its higher order terms are ignored, enabling the state equation to be written into an augmented form [24], [25]. Although the method of compensator can weaken the influence of time delay, it needs to establish an accurate model of the controlled object. However, its robust performance is relatively poor. The other method is to include the actuator time delay into the controller design process [26], [27] and to design a controller that can robustly stabilize the system and guarantee the system performance, in spite of the time delay existence. Due to the uncertainty and nonlinearity of suspension systems, it is necessary to design a robust controller to improve the performance of MRSS. The sliding mode variable structure control makes the system state move along the sliding surface, through the switching of control variables, which is invariant to the parameter perturbation and disturbance of MRSS. In the early years, Yokoyama *et al.* [28] conducted the sliding mode control on MRSS, by employing the proposed Bouc-Wen hysteresis model of the MRD and ideal skyhook suspension system as the control reference model. Pan [29] and Deshpande [30] considered a two-degree-of-freedom model as the research object and studied the influence of the switching coefficient of the sliding mode surface on the control effect of active suspension. Based on the aforementioned prior knowledge, in order to achieve better robust performance, Wang and Zhao [31] studied an intelligent second order sliding mode control method, combining second-order sliding mode control and Recurrent Radial Basis Function Neural Network (RRBFNN). However, the lack of consideration for time delay, as well as the absence of analysis of the effect of time delay on the system stability, motivate this study of a controller design that can robustly stabilize the system, in spite of the existence of time delay.

Based on the prior literature survey, the time delay dependent controller can ensure the stability of MRSS system and still show good robustness and control performance, in the case of time delay. However, calculating the critical time delay of the MRSS system, while ensuring that it lies within the critical time delay range, is the key problem of controller design. In this paper, a delay dependent sliding mode variable structure controller for MRSS with time delay is proposed. Based on the method of Linear Matrix Inequality (LMI), the asymptotic stability problem of sliding mode is transformed into a feasibility problem, which can be solved by the solver 'feasp' in the LMI toolbox. In addition, the calculation of critical time delay of a semi-active suspension system is also expressed as a generalized eigenvalue optimization problem. The remainder of this paper is organized as follows. In Section II, the problem is formulated. In Section III, a delay dependent sliding mode variable structure controller is proposed, for MRSS with time delay, while the delay stability condition and the calculation method of critical delay are provided by using LMI. In Section IV, the time delay measurement of MRD is carried out. In Section V, the proposed MRSS control system is simulated and verified. In Section VI, real vehicle tests are presented. Finally, conclusions are included in Section VII.

II. MAGNETO-RHEOLOGICAL TIME DELAY SEMI-ACTIVE SUSPENSIONMODEL

A. MRD MODEL

The dynamic performance test of MRD shows that, the output force of MRD can be expressed by piston rod displacement and velocity, showing very strong nonlinear characteristics. The Sigmoid model is proposed to describe the nonlinear hysteretic characteristics of MRD [32], as shown in Fig.1.

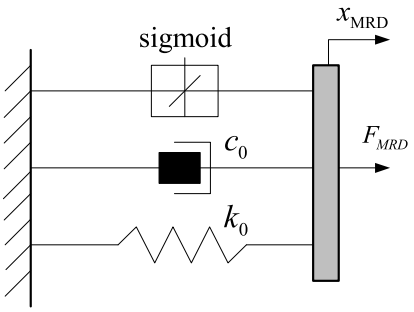

FIGURE 1. Sigmoid model.

Here, ignoring the shear thinning occurrence and inertia effect of magneto-rheological fluid, the mechanical model of MRD can be expressed by the following formula:

$$F_{MRD} = F_0 \frac{1 - e^{-a(\dot{x}_{MRD}+k_0 x_{MRD})}}{1 + e^{-a(\dot{x}_{MRD}+k_0 x_{MRD})}} + C_0(\dot{x}_{MRD}+k_0 x_{MRD})+f_0 \tag{1}$$

where,F_{MRD} represents the damping force of MRD,F_0 is the maximum yield stress,a represents the parameter related to the damping coefficient in the pre yield zone,C_0 is the parameter related to the damping characteristics of the post yield zone,k_0 represents the hysteresis loop width scale factor,f_0 refers to the offset damping force and x_{MRD} is the dynamic stroke of MRD.

The F_0 and C_0 are related to the MRD coil current, which can be calculated, according to the nonlinear least square method.

$$\begin{cases} F_0 = b_1 I + c_1 \\ C_0 = b_2 I + c_2 \end{cases} \tag{2}$$

where,I represents the current of damper coil;b_1, b_2, c_1, c_2 represent the characteristic parameters of MRD.

B. SEMI-ACTIVE SUSPENSION MODEL

Since the MRD actuator consists of mechanical and hydraulic systems, unavoidable time delays are encountered in real applications. In addition, time delays may appear in the control channel, particularly in the digital controller, as it carries out the complex calculations associated with the control law, as well as the process of collection and transmission of sensor signal. Compared to the actuator time delay, the one caused by signal collection/transmission and control law calculation is extremely small. Therefore, this paper only considers the influence of actuator time delay, on the performance of the MRSS control system. A two degree of freedom quarter vehicle MRSS model with actuator response time delay is established, as shown in Fig.2. This model has been used extensively in the literature, because it can capture many important characteristics of complicated suspension models.

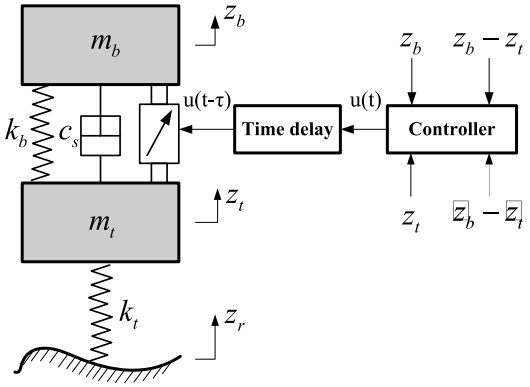

FIGURE 2. Semi-active suspension model.

The dynamic equation of a vehicle semi-active suspension system is expressed as follows:

$$\begin{cases} m_b\ddot{z}_b + k_b(z_b - z_t) + c_s(\dot{z}_b - \dot{z}_t) \\ \quad +F_{MRD}(t-\tau)sgn(\dot{z}_b - \dot{z}_t) = 0 \\ m_t\ddot{z}_t - k_b(z_b - z_t) + k_t(z_t - z_r) - c_s(\dot{z}_b - \dot{z}_t) \\ \quad -F_{MRD}(t-\tau)sgn(\dot{z}_b - \dot{z}_t) = 0 \end{cases} \tag{3}$$

where,z_b refers to the vertical displacement of a sprung mass,z_t refers to the vertical displacement of a non-sprung mass,$\dot{z}_b$ and $\ddot{z}_b$ refer to vertical velocity and acceleration of a sprung mass,$\dot{z}_t$ and $\ddot{z}_t$ refer to the vertical velocity and acceleration of a non-sprung mass,m_b refers to the sprung mass,m_t refers to the non-sprung mass,k_b refers to the suspension spring stiffness,k_t refers to the tire stiffness,z_r refers to the road excitation,τ refers to the time delay of system control input.

By defining the state variable $\mathbf{X} = \left[z_b \;\; z_b - z_t \;\; \dot{z}_b \;\; \dot{z}_b - \dot{z}_t \right]^T$ and output variable $\mathbf{Y} = \left[\ddot{z}_b \;\; z_b - z_t \;\; z_t - z_r \right]^T$,the state space equation of MRSS is expressed as:

$$\begin{cases} \dot{\mathbf{X}}(t) = \mathbf{A}\mathbf{X}(t) + \mathbf{B}u(t-\tau) + \mathbf{E}z_r(t) \\ \mathbf{Y}(t) = \mathbf{C}\mathbf{X}(t) + \mathbf{D}u(t-\tau) + \mathbf{G}z_r(t) \end{cases} \tag{4}$$

where, $\mathbf{A}$, $\mathbf{B}$, $\mathbf{E}$, $\mathbf{C}$, $\mathbf{D}$, $\mathbf{G}$, and $u(t)$, as shown at the bottom of the next page.

III. TIME DELAY-DEPENDENT SLIDING MODE CONTROLLER DESIGN

In the MRSS control system, time delay is inevitable. In this article, a delay dependent sliding mode variable structure controller is designed, to compensate for the time delay, reducing its negative impact on the control performance. The control law is directly derived from delay differential equations, so this method is easy to ensure the stability of the control system. The schematic diagram of the MRSS control system is shown in Fig.3.

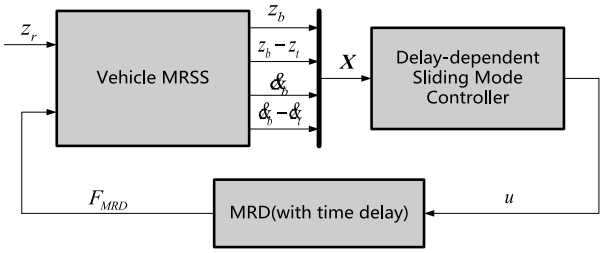

FIGURE 3. The schematic diagram of the MRSS control system.

A. SLIDING MODE CONTROLLER DESIGN

A control input time delay is found in the systems described by Eq.(4). This delay increases the difficulty of the sliding mode design. A switching functional with sliding mode compensator is constructed, to overcome this difficulty as follows:

$$s = \mathbf{H}X + \int_{t-\tau}^{t} \mathbf{HB}u(t-\xi)d\xi + \mathbf{P} \tag{5}$$

where,$\mathbf{H}$ is a 1×4 constant matrix to be calculated;$\mathbf{P}$ is a sliding mode compensator with the following mathematical model:

$$\dot{\mathbf{P}} = -\mathbf{H}(\mathbf{A} + \mathbf{B}K)\mathbf{X} \tag{6}$$

where,$\mathbf{K}$ is a constant matrix related to the value of time delay. The existence and reach ability conditions of sliding mode can be classified as generalized sliding mode conditions $s\dot{s} < 0$. The following exponential reaching law can be used to improve the dynamic quality of reaching motion, as follows:

$$\dot{s} = -\alpha f_{sat}(\frac{s}{\mu}) - \beta s \tag{7}$$

where,α refers to the convergence velocity and β refers to the arrival velocity. The function f_{sat} is defined as follows:

$$f_{sat}(\frac{s}{\mu}) = \begin{cases} 1 & s > \mu \\ s/\mu & -\mu \le s \le \mu \\ -1 & s < -\mu \end{cases} \tag{8}$$

where,μ refers to the boundary layer thickness. The differentiation of switching functional along the trajectories of system states can be expressed in the following form:

$$\dot{s} = \mathbf{H}\dot{\mathbf{X}} + \mathbf{HB}u(t-\tau) + \dot{\mathbf{P}} \tag{9}$$

In accordance with Eqs. (6), (7) and (9), the following formula is obtained:

$$\mathbf{HB}u - \mathbf{HBKX} + \mathbf{HE}z_r = -\alpha f_{sat}(\frac{s}{\mu}) - \beta s \tag{10}$$

Therefore, the sliding mode control law u is obtained as:

$$u = \mathbf{KX} - [\mathbf{HB}]^{-1}\left[\mathbf{HE}z_r + \alpha f_{sat}(\frac{s}{\mu}) + \beta s\right] \tag{11}$$

Under the control law described in Eq. (11), the sliding mode equation of MRSS can be expressed as follows:

$$\dot{\mathbf{X}} = \mathbf{AX} + \mathbf{BKX}(t-\tau) + \mathbf{E}(z_r(t) - z_r(t-\tau)) \tag{12}$$

The parameter matrix $\mathbf{K}$ is related to the time delay of the system. Therefore, the control law in Eq. (11) is a delay dependent sliding mode controller. In the following, the existence and stability conditions of sliding mode of the system are derived by using LMI, while the calculation method of the critical time delay for the stability of MRSS is given.

B. SYSTEM STABILITY ANALYSIS

The sliding mode in Eq. (12) can be rewritten as follows:

$$\dot{\mathbf{X}} = (\mathbf{A} + \mathbf{B}K) - \mathbf{BK}\int_{t-\tau}^{t} \dot{x}(\theta)d\theta + \mathbf{E}\delta \tag{13}$$

where,$\delta = z_r(t) - z_r(t-\tau)$.

The Lyapunov-Krasovskii functional is defined as follows:

$$V = \mathbf{X}^T(t)\mathbf{GX}(t) + \int_{-\tau}^{0}\int_{t+\eta}^{t} \dot{\mathbf{X}}^T(\xi)\mathbf{Z}\dot{\mathbf{X}}(\xi)d\xi d\eta + \int_{t-\tau}^{t} \mathbf{X}^T(\xi)\mathbf{QX}(\xi)d\mu \tag{14}$$

$$\mathbf{A} = \begin{bmatrix} 0 & 0 & 1 & 0 \\ 0 & 0 & 0 & 1 \\ 0 & -k_b/m_b & 0 & -c_s/m_b \\ k_t/m_t & -k_b/m_t - k_t/m_t - k_b/m_b & 0 & -c_s/m_t - c_s/m_b \end{bmatrix}$$

$$\mathbf{B} = \begin{bmatrix} 0 & 0 & -1/m_b & -1/m_b - 1/m_t \end{bmatrix}^T$$

$$\mathbf{E} = \begin{bmatrix} 0 & 0 & 0 & -k_t/m_t \end{bmatrix}^T$$

$$\mathbf{C} = \begin{bmatrix} 0 & -k_b/m_b & 0 & -c_s/m_b \\ 0 & 1 & 0 & 0 \\ 1 & -1 & 0 & 0 \end{bmatrix}$$

$$\mathbf{D} = [\,1/m_b \;\; 0 \;\; 0\,]^T$$

$$\mathbf{G} = [\,0 \;\; 0 \;\; -1\,]^T$$

$$u(t) = F_{MRD}(t)sgn(\Delta v).$$

where,$\mathbf{G}$, $\mathbf{Z}$, and $\mathbf{Q}$ are 4×4 dimensional positive definite matrices. The differential equation of V can be written as follows:

$$\begin{aligned}\dot{V} \leq\ & \mathbf{X}^T[\mathbf{A}^T\mathbf{G} + \mathbf{G}\mathbf{A} + \tau\mathbf{X} + \mathbf{Y} + \mathbf{Y}^T]\mathbf{X} + \delta^T\mathbf{E}^T\mathbf{P}\mathbf{X} \\ & + 2\mathbf{X}^T[\mathbf{G}\mathbf{B}\mathbf{K} - \mathbf{Y}]\mathbf{X}(t-\tau) + \mathbf{X}^T\mathbf{P}\mathbf{E}\delta + \mathbf{X}^T\mathbf{Q}\mathbf{X} \\ & + \mathbf{X}^T(t-\tau)[\mathbf{K}^T\mathbf{B}^T\mathbf{G} - \mathbf{Y}^T]\mathbf{X} - \mathbf{X}^T(t-\tau)\mathbf{Q}\mathbf{X}(t-\tau) \\ & + \tau\,[\mathbf{A}\mathbf{X} + \mathbf{B}\mathbf{K}\mathbf{X}(t-\tau) + \mathbf{E}\delta]^T \\ & \times\mathbf{Z}\,[\mathbf{A}\mathbf{X} + \mathbf{B}\mathbf{K}\mathbf{X}(t-\tau) + \mathbf{E}\delta] \\ =\ & \left[\mathbf{X}\ \mathbf{X}(t-\tau)\ \delta\right]\Psi\left[\mathbf{X}\ \mathbf{X}(t-\tau)\ \delta\right]^T \end{aligned} \tag{15}$$

where, Ψ, as shown at the bottom of the page. If $\Psi < 0$, then $\dot{V} < 0$. Thus, the sliding mode of the system, as described in Eq. (12), is asymptotically stable. In accordance with Schur complement matrix property, the matrix inequality $\Psi < 0$ can be rewritten as follows (16), as shown at the bottom of the page.

The matrix $diag\left\{\mathbf{G}^{-1}\ \mathbf{G}^{-1}\ \mathbf{I}\ \mathbf{Z}^{-1}\right\}$ is multiplied on the left and right sides of matrix inequality in Eq. (16). I is a 4×4 unit matrix. Eq.(16) is rewritten as follows (17), as shown at the bottom of the page, where,$\Phi = \mathbf{G}^{-1}\mathbf{A}^T + \mathbf{A}\mathbf{G}^{-1} + \tau\mathbf{G}^{-1}\mathbf{X}\mathbf{G}^{-1} + \mathbf{G}^{-1}\mathbf{Y}\mathbf{G}^{-1} + \mathbf{G}^{-1}\mathbf{Y}^T\mathbf{G}^{-1} + \mathbf{G}^{-1}\mathbf{Q}\mathbf{G}^{-1}$.

Considering the definitions: $\mathbf{L} = \mathbf{G}^{-1}$, $\mathbf{M} = \mathbf{K}\mathbf{L}$, $\mathbf{N} = \mathbf{L}\mathbf{X}\mathbf{L}$, $\mathbf{J} = \mathbf{L}\mathbf{Y}\mathbf{L}$, $\mathbf{S} = \mathbf{L}\mathbf{Q}\mathbf{L}$, and $\mathbf{T} = \mathbf{Z}^{-1}$, Eq.(17) can be transformed into the following formula (18), as shown at the bottom of the page.

If there is a 4×4 matrix L, N, S, and $\mathrm{M} \in R^{1\times4}$, $\mathrm{J} \in R^{4\times4}$, for any time delay satisfying $0 \leq \tau \leq \tau_c$, $\mathrm{K} = \mathrm{ML}^{-1}$ is considered correct. The sliding mode in Eq. (12) is asymptotically stable, while τ_c is the critical time delay of vehicle MRSS system. By using Lyapunov-Krasovskii functional, the time delay control strategy, meeting the stability of closed-loop system requirement, is designed, while the respective conditions are derived. Compared to sliding mode controller with time delay compensator, the time delay dependent sliding mode controller can robustly stabilize the system and guarantee the system performance, despite the existence of time delay. In order to solve the gain matrix K, the above conditions are transformed into equivalent linear matrix inequalities, which is easier to calculate and solve.

C. CALCULATION OF CRITICAL TIME DELAY

The critical time delay is the critical point, where a time delay system changes from an asymptotically stable state to an unstable state. It is the maximum allowable delay time, while the system maintains a stable state. The critical delay of the MRSS control system in Eq. (4) can be obtained by solving the following optimization problems (19), as shown at the bottom of the next page.

The global optimal solution of Eq. (19) can be obtained by using the solver 'gevp' in LMI toolbox. In accordance with the Schur complement matrix property, the above optimization problem in Eq. (19) can be transformed into the following generalized eigenvalue minimization problem (20), as shown at the bottom of the next page.

The global optimal solution γ of the above optimization problem in Eq. (20) is also obtained by using the solver 'gevp' in LMI toolbox, while the critical time delay $\tau_c = 1/\gamma$.

IV. TIME DELAY MEASUREMENT OF MRD

In order to verify the feasibility and mechanical characteristics of MRD, as an actuator of automotive semi-active suspension, the prototype of MRD is produced. According

$$\Psi = \begin{bmatrix} \mathbf{A}^T\mathbf{G} + \mathbf{G}\mathbf{A} + \tau\mathbf{X} + \mathbf{Y} + \mathbf{Y}^T + \mathbf{Q} + \tau\mathbf{A}^T\mathbf{Z}\mathbf{A} & \mathbf{G}\mathbf{B}\mathbf{K} - \mathbf{Y} + \tau\mathbf{A}^T\mathbf{Z}\mathbf{B}\mathbf{K} & \mathbf{G}\mathbf{E} + \tau\mathbf{A}^T\mathbf{Z}\mathbf{E} \\ \mathbf{K}^T\mathbf{B}^T\mathbf{G} - \mathbf{Y}^T + \tau\mathbf{K}^T\mathbf{B}^T\mathbf{Z}\mathbf{A} & \tau\mathbf{K}^T\mathbf{B}^T\mathbf{Z}\mathbf{B}\mathbf{K} - \mathbf{Q} & \tau\mathbf{K}^T\mathbf{B}^T\mathbf{Z}\mathbf{E} \\ \mathbf{E}^T\mathbf{G} + \tau\mathbf{E}^T\mathbf{Z}\mathbf{A} & \tau\mathbf{E}^T\mathbf{Z}\mathbf{B}\mathbf{K} & \tau\mathbf{E}^T\mathbf{Z}\mathbf{E} \end{bmatrix}$$

$$\begin{bmatrix} \mathbf{A}^T\mathbf{G} + \mathbf{G}\mathbf{A} + \tau\mathbf{X} + \mathbf{Y} + \mathbf{Y}^T + \mathbf{Q} & \mathbf{G}\mathbf{B}\mathbf{K} - \mathbf{Y} & \mathbf{G}\mathbf{E} & \tau\mathbf{A}^T\mathbf{Z} \\ \mathbf{K}^T\mathbf{B}^T\mathbf{G} - \mathbf{Y}^T & -\mathbf{Q} & 0 & \tau\mathbf{K}^T\mathbf{B}^T\mathbf{Z} \\ \mathbf{E}^T\mathbf{G} & 0 & 0 & \tau\mathbf{E}^T\mathbf{Z} \\ \tau\mathbf{Z}\mathbf{A} & \tau\mathbf{Z}\mathbf{B}\mathbf{K} & \tau\mathbf{Z}\mathbf{E} & -\tau\mathbf{Z} \end{bmatrix} < 0 \tag{16}$$

$$\begin{bmatrix} \Phi & \mathbf{B}\mathbf{K}\mathbf{G}^{-1} - \mathbf{G}^{-1}\mathbf{Y}\mathbf{G}^{-1} & \mathbf{E} & \tau\mathbf{G}^{-1}\mathbf{A}^T \\ \mathbf{G}^{-1}\mathbf{K}^T\mathbf{B}^T - \mathbf{G}^{-1}\mathbf{Y}^T\mathbf{G}^{-1} & -\mathbf{G}^{-1}\mathbf{Q}\mathbf{G}^{-1} & 0 & \tau\mathbf{G}^{-1}\mathbf{K}^T\mathbf{B}^T \\ \mathbf{E}^T & 0 & 0 & \tau\mathbf{E}^T \\ \tau\mathbf{A}\mathbf{G}^{-1} & \tau\mathbf{B}\mathbf{K}\mathbf{G}^{-1} & \tau\mathbf{E} & -\tau\mathbf{Z}^{-1} \end{bmatrix} \tag{17}$$

$$\begin{bmatrix} \mathbf{L}\mathbf{A}^T + \mathbf{A}\mathbf{L} + \tau\mathbf{N} + \mathbf{J} + \mathbf{J}^T + \mathbf{S} & \mathbf{B}\mathbf{M} - \mathbf{J} & \mathbf{E} & \tau\mathbf{L}\mathbf{A}^T \\ \mathbf{M}^T\mathbf{B}^T - \mathbf{J}^T & -\mathbf{S} & 0 & \tau\mathbf{M}^T\mathbf{B}^T \\ \mathbf{E}^T & 0 & 0 & \tau\mathbf{E}^T \\ \tau\mathbf{A}\mathbf{L} & \tau\mathbf{B}\mathbf{M} & \tau\mathbf{E} & -\tau\mathbf{T} \end{bmatrix} < 0 \tag{18}$$

to the test method of automobile shock absorber, the time delay measurement of MRD is carried out on material testing machine, as shown in Fig.4.

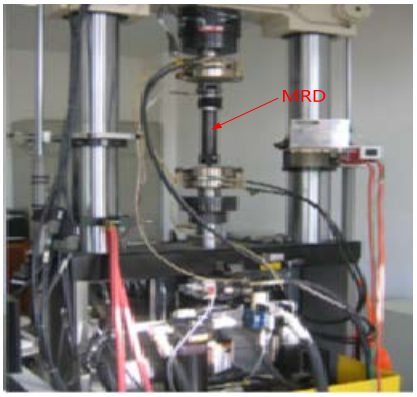

FIGURE 4. MRD time delay test.

The amplitude of material testing machine is set at 25mm, the frequency is at 0.4Hz and the loading mode has the form of a triangular wave. In the stretching stroke of the shock absorber, the current input to the MRD coil is regulated between 0-0.5A, 0-1.0A, 0-1.5A, 0-2.0A, where as the damping force of MRD, from one steady state to another, is measured. The test results are shown in Fig.5.

The time delay of MRD is defined as the time required for the initial damping force to reach 95% of the steady state damping force [33]. The results, as derived from Fig.5, are listed in Tables1 and 2.

Tables 1 and 2 show that, the change of coil current range has little effect on the time delay of MRD. The time delay of current increase is obviously less than that of current decrease, which is mainly caused by the residual magnetism in the magnetic circuit of the MRD. The existence of the residual magnetic field hinders the rapid decline of the damping force of the damper. The test results show that, the time delay of the designed MRD is no more than 28ms and it shows fast dynamic response speed.

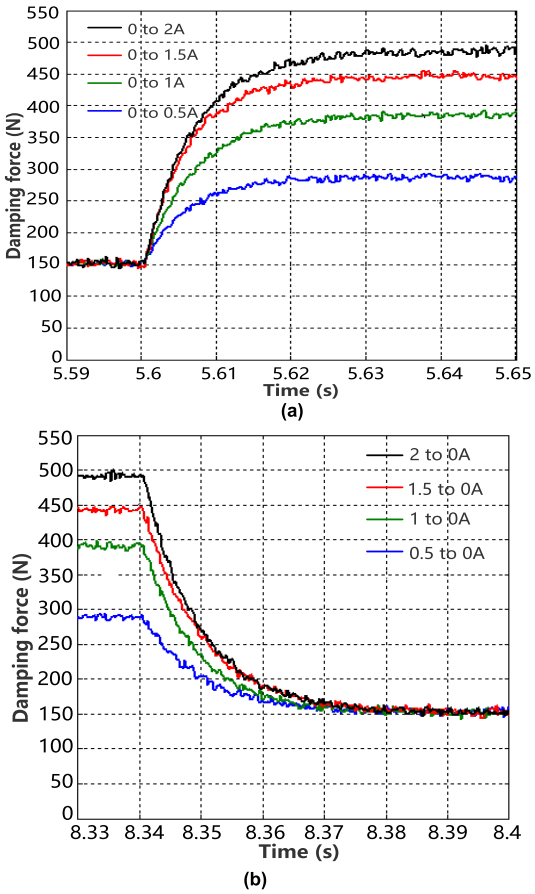

FIGURE 5. Damping force under different coil currents. (a) Coil current increase. (b) Coil current decrease.

$$\begin{aligned}
&\max_{\mathbf{L},\mathbf{M},\mathbf{N},\mathbf{J},\mathbf{S},\mathbf{T}} \tau \\
&s.t.\ \mathbf{L}>0, \mathbf{N}>0, \mathbf{S}>0, \begin{bmatrix} \mathbf{N} & \mathbf{J} \\ \mathbf{J}^T & \mathbf{L} \end{bmatrix} \geq 0 \\
&\begin{bmatrix} \mathbf{L}\mathbf{A}^T+\mathbf{A}\mathbf{L}+\tau\mathbf{N}+\mathbf{J}+\mathbf{J}^T+\mathbf{S} & \mathbf{B}\mathbf{M}-\mathbf{J} & \mathbf{E} & \tau\mathbf{L}\mathbf{A}^T \\ \mathbf{M}^T\mathbf{B}^T-\mathbf{J}^T & -\mathbf{S} & 0 & \tau\mathbf{M}^T\mathbf{B}^T \\ \mathbf{E}^T & 0 & 0 & \tau\mathbf{E}^T \\ \tau\mathbf{A}\mathbf{L} & \tau\mathbf{B}\mathbf{M} & \tau\mathbf{E} & -\tau\mathbf{L} \end{bmatrix} < 0
\end{aligned} \tag{19}$$

$$\begin{aligned}
&\min \gamma \\
&s.t.\ \begin{bmatrix} \mathbf{N} & \mathbf{J} \\ \mathbf{J}^T & \mathbf{L} \end{bmatrix} \geq 0 \\
&\begin{bmatrix} \mathbf{L}\mathbf{A}^T \\ \mathbf{M}^T\mathbf{B}^T \\ \mathbf{E}^T \end{bmatrix} \mathbf{L}^{-1} \begin{bmatrix} \mathbf{L}\mathbf{A}^T \\ \mathbf{M}^T\mathbf{B}^T \\ \mathbf{E}^T \end{bmatrix}^T < -\gamma \begin{bmatrix} \mathbf{L}\mathbf{A}^T+\mathbf{A}\mathbf{L}+\tau\mathbf{N}+\mathbf{J}+\mathbf{J}^T+\mathbf{S} & \mathbf{B}\mathbf{M}-\mathbf{J} & \mathbf{E} \\ \mathbf{M}^T\mathbf{B}^T-\mathbf{J}^T & -\mathbf{S} & 0 \\ \mathbf{E}^T & 0 & 0 \end{bmatrix} \\
&\mathbf{L}>0, \mathbf{N}>0, \mathbf{S}>0
\end{aligned} \tag{20}$$

TABLE 1. Time delay with increasing coil current.

Coil current (A)	0 to 0.5	0 to 1	0 to 1.5	0 to 2
Time delay (ms)	20.7	22.4	20.3	21.6

TABLE 2. Time delay with decreasing coil current.

Coil current (A)	0.5 to 0	1 to 0	1.5 to 0	2 to 0
Time delay (ms)	26.4	25.6	27.7	26.8

V. SIMULATION VALIDATION

In order to verify the effectiveness of the proposed control system and the controller, the model is simulated using MATLAB/Simulink software, under two different road conditions. Table 3 shows the parameters of the MRSS.

TABLE 3. Semi-active suspension parameters.

Symbol	Parameters	Values
m_b	Sprung mass	320 kg
m_t	Non-sprung mass	40 kg
k_b	Spring stiffness	20 kN/m
k_t	Tire stiffness	220 kN/m
c_s	Damping coefficient	1317 N/m.s^{-1}
a, F_0, k_0	MRD parameters	843.72,6.99,0.31
b_1, b_2, c_1, c_2	MRD coefficient	119.01,451.67,40.78,161.85

For convenience purposes, the delay dependent sliding mode controller is referred to as controller I. The controller parameters are $\mathrm{H} = \begin{bmatrix} 14.28 & -1.25 & 0 & 35.6 \end{bmatrix}$, $\alpha = 0.15$, $\beta = 34$, and $\mu = 0.01$. The critical time delay of the MRSS system is obtained as $\tau_c = 32.4ms$, by using 'gevp' in the LMI toolbox, to solve the optimization problem in Eq. (20). In accordance with the test results, the time delay of MRD is 28 ms, which is less than the critical time delay. The solver 'feasp' in LMI toolbox is used to solve Eq.(18), while the delay dependent sliding mode controller $\mathrm{K} = \begin{bmatrix} -198.14 & 182.06 & 19.87 & -3.67 \end{bmatrix}$. In the simulation, it is assumed that the actuator shows time delay and a sliding mode variable structure controller without time delay is designed. In the comparison, this controller is called controller II. Moreover, in the following simulation and real vehicle test, smith compensation method for time delay is used as a comparative analysis.

A. BUMP PULSE ROAD

The bump pulse road simulation was used to analyze the suppression effect of time delay dependent sliding mode control on bump vibration. In the simulation, the vehicle passes over the single bump at $v = 40$km/h speed. The single bump model can be expressed as follows:

$$x_r(t) = \begin{cases} \frac{\lambda}{2}(1 - \cos(\frac{2\pi v}{l}t)) & 0 \le t \le \frac{l}{v} \\ 0 & t > \frac{l}{v} \end{cases} \quad (21)$$

where,$\lambda = 0.06$m, $l = 2$m.

The curves of sprung mass acceleration, suspension dynamic deflection and tire dynamic displacement are shown in Figs. 6, 7 and 8, respectively. After the pulse signal is administered, the sprung mass acceleration, suspension dynamic deflection and tire dynamic displacement increase sharply, followed by a rapid attenuation under the effect of damping. However, the low frequency oscillation is still active for some time.

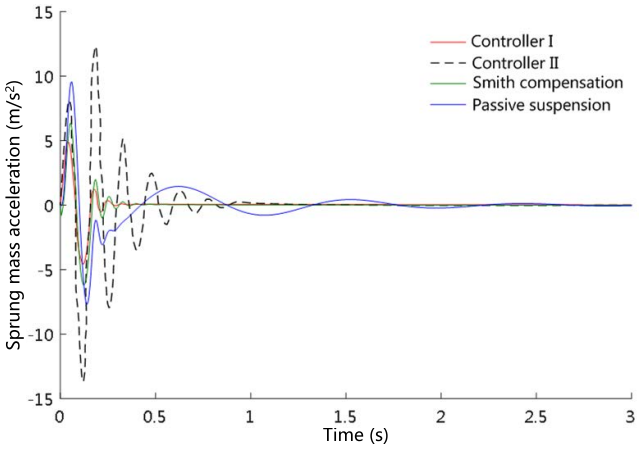

FIGURE 6. Sprung mass acceleration.

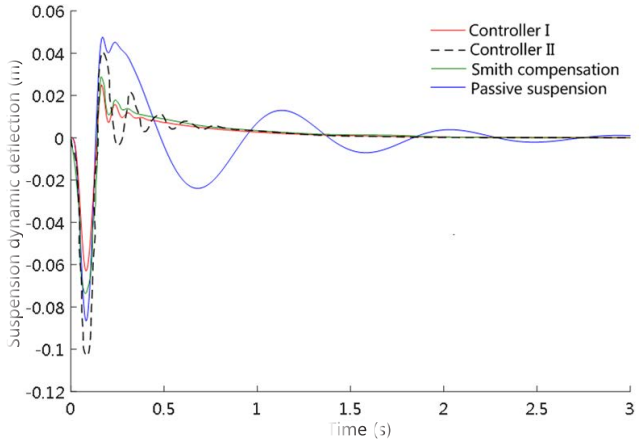

FIGURE 7. Suspension dynamic deflection.

Table 4 shows the results of road bump pulse simulation, where the sprung mass acceleration, suspension dynamic deflection and tire dynamic displacement, under the action of controller I, are reduced by 23.76%, 35.34% and 51.37%, respectively, while the adjustment time of the transition process is short, compared to the one of passive suspension. Although the adjustment time of controller II is shorter than in passive suspension, its peak value is higher than that of

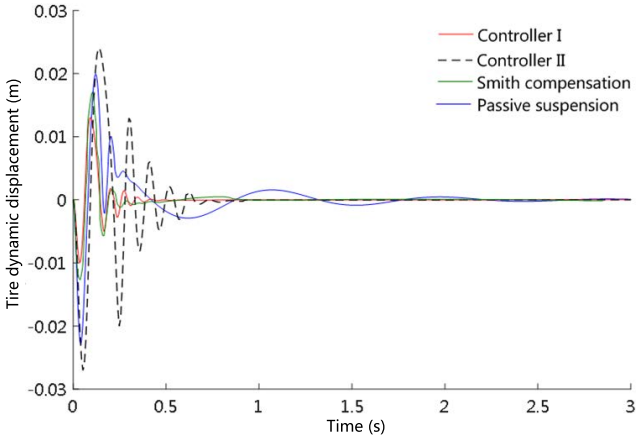

FIGURE 8. Tire dynamic displacement.

TABLE 4. Simulation results of road bump pulse.

Parameters	Controller	Peak value	Adjustment time (s)
Sprung mass acceleration(m/s^2)	Passive suspension	9.85	1.48
	Controller I	4.86	0.26
	Controller II	14.12	0.72
	Smith compensation	6.22	0.43
Suspension dynamic deflection(cm)	Passive suspension	8.22	1.61
	Controller I	6.17	0.82
	Controller II	10.54	0.95
	Smith compensation	7.42	0.85
Tire dynamic displacement(cm)	Passive suspension	2.55	1.68
	Controller I	1.24	0.3
	Controller II	2.62	0.82
	Smith compensation	1.58	0.32

passive suspension by 43.35%, 28.22% and 2.75%. The delay dependent sliding mode controller can reduce the vehicle peak response and shorten the time needed to attenuate the bump pulse effect, in the spite of time delay.

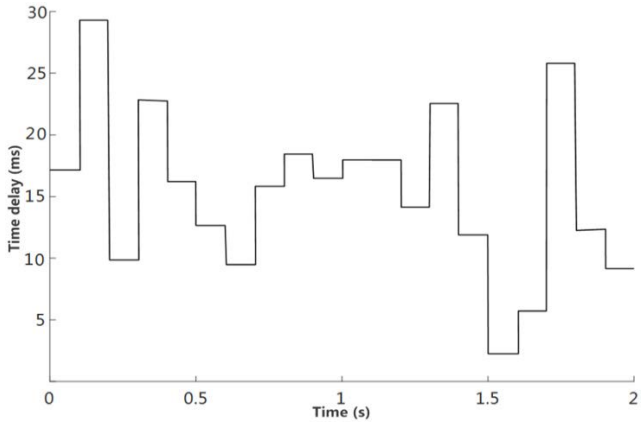

FIGURE 9. Random and time-varying delay.

The white noise, as shown in Fig. 9, is used to simulate the random and time-varying delay of MRSS control loop, where the upper limit of maximum delay is less than 30ms. The effect of time-varying delay on the sprung mass acceleration

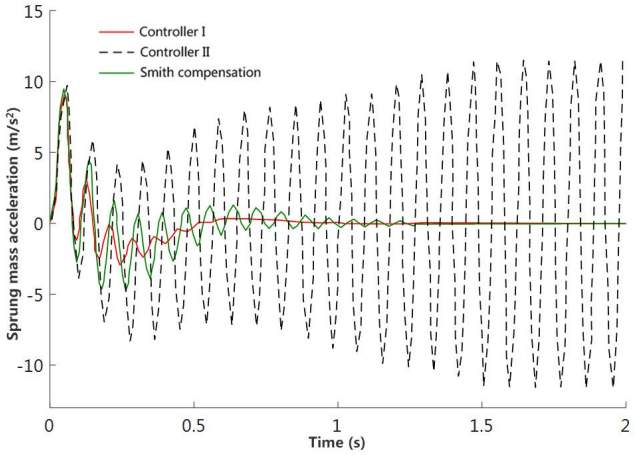

FIGURE 10. Sprung mass acceleration.

is illustrated in Fig.10. Even in the case of input time-varying delay, the controller I can still effectively improve the comfort of the vehicle. The controller shows strong robustness to the influence of input time delay.

B. RANDOM ROAD

The random road model can be expressed as follows [34]:

$$\dot{x}_r(t) = -2\pi g_0 x_r(t) + 2\pi\sqrt{G_0 v}\theta(t) \tag{22}$$

where, the road surface unevenness factor of G_0 is 64×10^{-6} and the vehicle speed is $v = 20$m/s. $\theta(t)$ is the Gaussian white noise with zero mathematical expectation and the lower cut-off frequency is $g_0 = 0.1$.

Figure11 shows the vertical acceleration of sprung mass. In the case of control input time delay, controller I exhibits good suppression effect, at the peak value of the sprung mass acceleration. However, the control quality of controller II on the sprung mass vertical acceleration is inferior to that of the passive suspension.

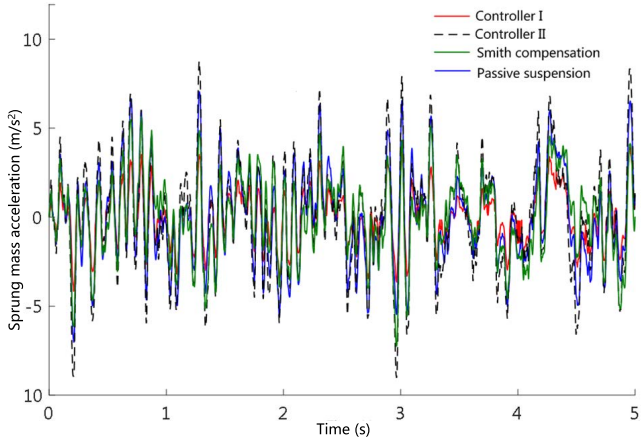

FIGURE 11. Sprung mass acceleration.

As shown in Fig. 12, the control input time delay mostly affects the first-order main mode. This condition indicates

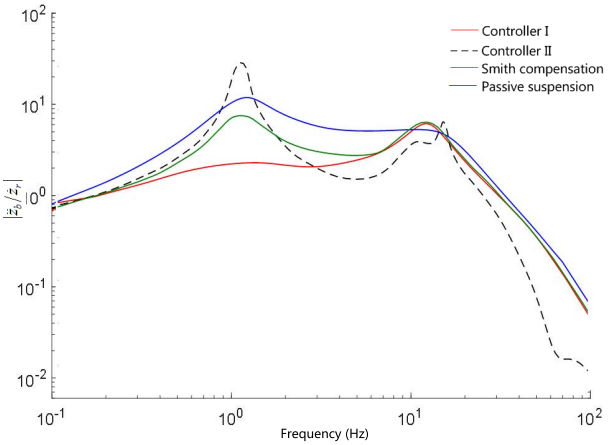

FIGURE 12. Amplitude frequency characteristic of sprung mass acceleration.

that, time delay has a great influence on the vibration of the vehicle body, but it shows far less influence on the vibration of the wheel. At a time delay of 28 ms, controller I reduces the first-order peak value of the sprung mass acceleration frequency characteristic by 56.8%, compared to the respective measure of the passive suspension. In the low-frequency resonance region, the peak value of controller II is 13.6% higher than that of passive suspension.

The dynamic deflection result of suspension is shown in Fig.13.

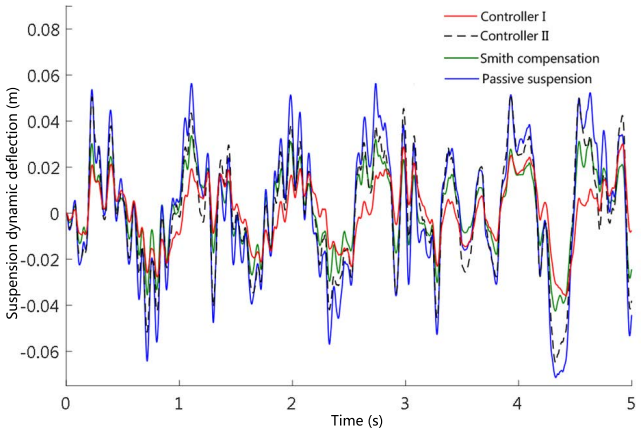

FIGURE 13. Suspension dynamic deflection.

Compared to controller II and smith compensation, the delay dependent sliding mode controller I can produce good control effect on the suspension dynamic deflection, even in the case where the control system shows time delay.

In random road simulation, in order to analyze the influence of time delays on the delay dependent sliding mode control performance, the Root Mean Square (RMS) responses of the sprung mass acceleration, suspension dynamic deflection and tire dynamic displacement at different time delay values, are listed in Tables 5, 6 and 7, as well as illustrated in Figs.14, 15 and 16.

TABLE 5. RMS response value (Controller I).

Time delay(ms)	Controller I		
	Sprung mass acceleration (m/s^2)	Suspension dynamic deflection(cm)	Tire dynamic displacement (cm)
0	0.37	0.65	0.18
5	0.4	0.68	0.19
10	0.42	0.71	0.2
15	0.45	0.74	0.21
20	0.49	0.78	0.21
25	0.5	0.79	0.22
30	0.51	0.79	0.22
35	0.85	1	0.34
40	1.54	1.13	0.41
45	2.79	1.39	0.58

TABLE 6. RMS response value (Controller II).

Time delay(ms)	Controller II		
	Sprung mass acceleration (m/s^2)	Suspension dynamic deflection(cm)	Tire dynamic displacement (cm)
0	0.37	0.65	0.18
5	0.42	0.72	0.2
10	0.47	0.77	0.21
15	0.59	0.8	0.22
20	0.71	0.82	0.23
25	0.9	0.83	0.31
30	1.21	0.91	0.33
35	1.51	1.22	0.4
40	1.88	1.46	0.49
45	3.66	1.98	0.62

TABLE 7. RMS response value (Smith compensation).

Time delay(ms)	Smith compensation		
	Sprung mass acceleration (m/s^2)	Suspension dynamic Deflection(cm)	Tire dynamic displacement (cm)
0	0.37	0.65	0.18
5	0.4	0.7	0.19
10	0.45	0.74	0.2
15	0.5	0.76	0.21
20	0.58	0.8	0.22
25	0.78	0.81	0.26
30	0.83	0.85	0.28
35	1.03	1.12	0.38
40	1.65	1.32	0.45
45	3.23	1.75	0.6

It is evident that, the RMS values of sprung mass acceleration, suspension dynamic deflection and tire dynamic displacement of MRSS increase along the rise of time delay. The control performance of the MRSS system finally deteriorates rapidly, when the time delay exceeds 30ms. Compared to controller II and smith compensation, controller I shows good robustness and control performance. At the time delay of 45ms, the RMS of sprung mass acceleration, suspension dynamic deflection and tire dynamic displacement for controller II reach 3.66 m/s^2, 1.98cm, 0.62cm, respectively, which seriously affects the ride comfort and handling stability of the vehicle. This occurs because

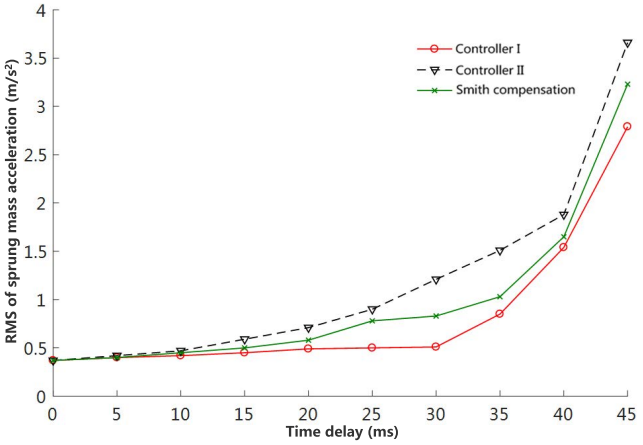

FIGURE 14. The RMS of Sprung mass acceleration.

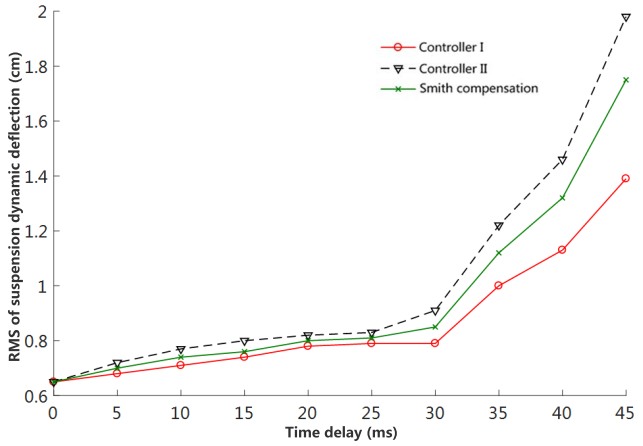

FIGURE 15. The RMS of suspension dynamic deflection.

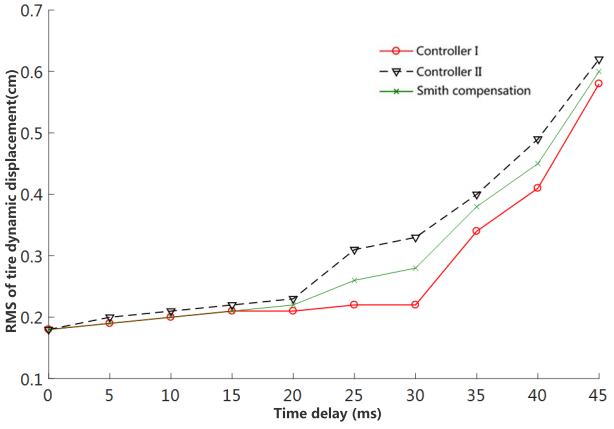

FIGURE 16. The RMS of tire dynamic displacement.

the controller II does not compensate for the time delay. As time delay increases, the RMS of the sprung mass acceleration increases accordingly, until it runs into the expected instability. Actually, the solution to the optimization problem in Eq. (20) provides the critical time delay value of the MRSS at 32.4ms. When the time delay is greater than the critical time delay, the stability of the sliding mode cannot be guaranteed, resulting in instability of the aforementioned delay dependent sliding mode control of MRSS system.

VI. REAL VEHICLE TEST VERIFICATION

A. TEST PLATFORM

Real vehicle test is conducted on a four-channel road simulation shaking machine, in order to verify the effectiveness of the control strategy. The instrument used in the test and the schematic of the test are shown in Fig.17.

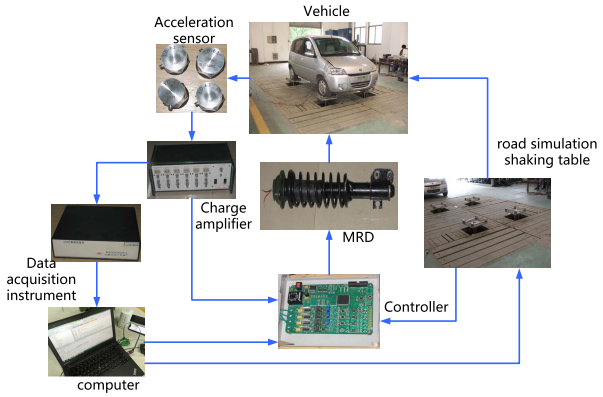

FIGURE 17. Real vehicle test system.

The real vehicle test system includes the vehicle, four acceleration sensors, charge amplifier, data acquisition instrument, a personal computer, a controller, a MRD and a road simulation shaking table. Two acceleration sensors are placed on the vehicle body, specifically mounted on the shock absorber, to measure the sprung mass vibration. One sensor is used to provide input signal to the controller, while the other is used to test the vibration state of the vehicle body. Another pair of acceleration sensors are placed on the lower control arm of the suspension, in order to measure the vibration of the non-sprung mass. As the test vehicle stands on the road simulation shaking table, the controller receives the signals from the force and displacement sensors, to calculate the tire dynamic load. In accordance with the acceleration sensor signals and the signals from the road simulation shaking table, the controller outputs 0–2A current to the MRD coil.

B. TEST RESULTS AND ANALYSIS

On the test platform, the control strategy of controllers I, controller II and smith compensation, are used to test the effectiveness of the proposed approach, under two road conditions. The real vehicle test parameters are the same as those in the simulation framework.

In the case of pulse road excitation, the sliding switching function of controllers I and II are illustrated in Fig.18. The illustration shows that, the sliding switching function of controller I converges to 0 at 0.4s, which can effectively attenuate the suspension vibration. The sliding switching function of controller II, without considering time delay, converges to 0 at 0.6s. The time delay dependent sliding mode

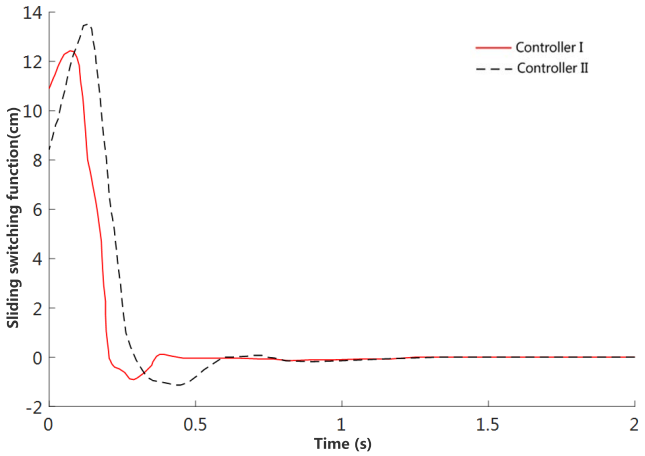

FIGURE 18. Sliding switching function.

controller shows a faster convergence speed, while reducing the adverse effect of time delay.

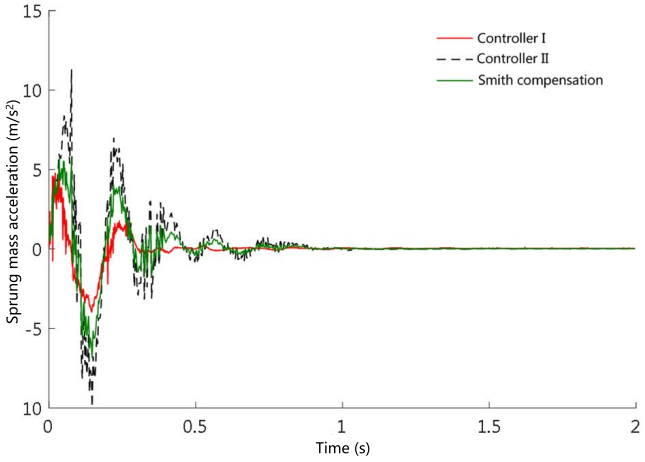

FIGURE 19. Sprung mass acceleration.

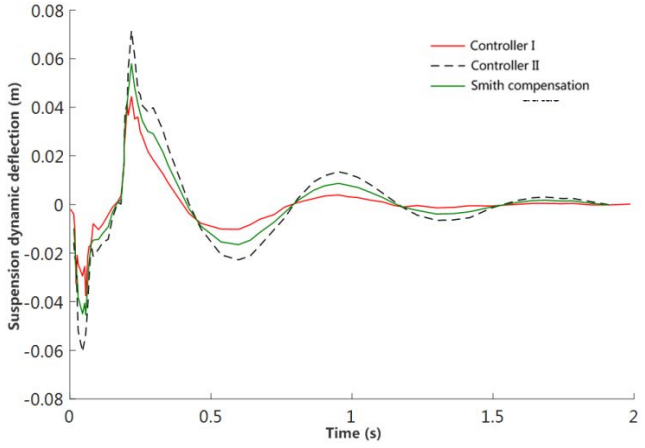

FIGURE 20. Suspension dynamic deflection.

The bump pulse road test results are shown in Figs. 19, 20 and 21. The controller I can reduce the peak value of vertical acceleration, from 11.6 m/s^2 to 4.98 m/s^2, while improving the performance by 57.8%. The peak value of suspension

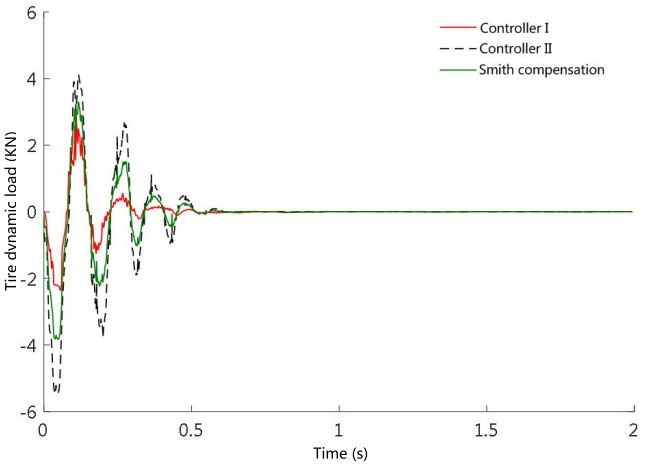

FIGURE 21. Tire dynamic load.

dynamic deflection is reduced by 42.6%, from 0.068m to 0.039m. The peak value of tire dynamic load is also well suppressed, while the adjustment time is significantly shorter than that of controller II.

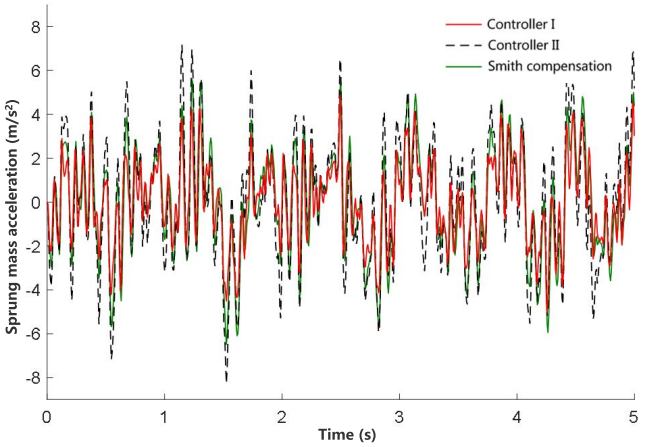

FIGURE 22. Sprung mass acceleration.

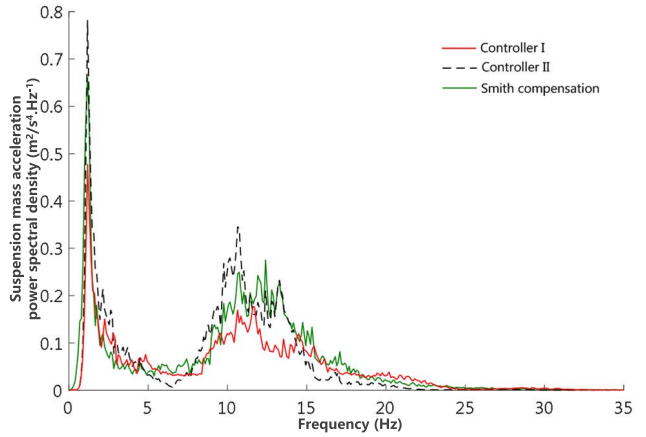

FIGURE 23. Power spectral density of sprung mass acceleration.

In the case of random road excitation with 10mm amplitude and 10 Hz signal bandwidth, the test results are shown in

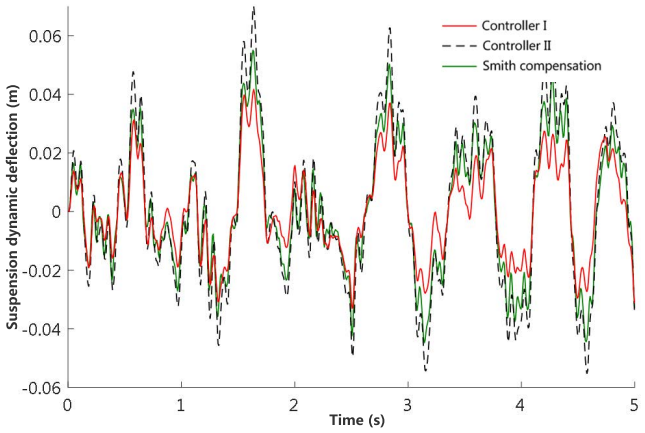

FIGURE 24. Suspension dynamic deflection.

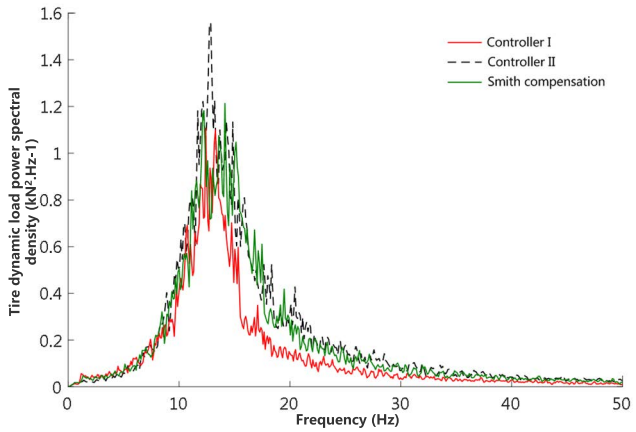

FIGURE 25. Power spectral density of tire dynamic load.

Figs. 22 to 25. Specifically, in Fig.22, the sprung mass acceleration of controller II appears to increase. Furthermore, through the time delay dependent sliding mode control strategy, the controller I can reduce the peak acceleration value.

The Power Spectral Density (PSD) of sprung mass acceleration is illustrated in Fig. 23.

In Fig.23, the result illustrates that controller I can reduce the PSD value of sprung mass acceleration, in spite of the existence of time delay, especially in the vicinity of the sprung mass resonant frequency (1.3Hz), indicating that the vehicle ride comfort can be improved. Regarding controller II and smith compensation, the energy vibration of the vehicle body and wheels increases significantly, as the wheel jump occurrence is observed.

In Fig.24, the suspension dynamic deflection peak value of controller I is 0.04m. The suspension dynamic deflection peak values of controller II and smith compensation are 0.075m and 0.058m, respectively, which leads to a more agitated suspension motion, and less ride comfort.

In Fig.25, the tire dynamic load PSD of controller I is significantly less than in the case of controller II and smith compensation, around the non-sprung mass natural frequency (13.2Hz), which implies that the vehicle road attachment and vehicle handling performance can also be improved by controller I.

TABLE 8. Sprung mass acceleration (RMS).

Controller	Test (m/s^2)	Simulation(m/s^2)
Controller I	0.46	0.51
Controller II	0.87	1.02
Smith compensation	0.65	0.73

TABLE 9. Suspension dynamic deflection (RMS).

Controller	Test (cm)	Simulation(cm)
Controller I	0.72	0.79
Controller II	0.87	0.91
Smith compensation	0.81	0.85

TABLE 10. Tire dynamic load (RMS).

Controller	Test (kN)	Simulation (kN)
Controller I	0.427	0.484
Controller II	0.663	0.705
Smith compensation	0.565	0.672

The random road test results are listed in Tables 8, 9 and 10. Compared to controller II, controller I reduces the RMS value of sprung mass acceleration, from 0.87 m/s^2 to 0.46 m/s^2, while it simproves the performance by 47.1%. The RMS value of suspension dynamic deflection is reduced from 0.87cm to 0.72cm, which means improvement by 17.2%. The RMS value of tire dynamic load is reduced, from 0.663 kN to 0.427 kN. The test results are slightly lower than those of the above simulation, due to the load change of the vehicle. The conclusion of the test is consistent with that of the simulation analysis. The real vehicle test results show that, the delay dependent sliding mode controller can ensure the stability of the system, overcome the influence of time delay on the control quality of MRSS and exhibits a good damping performance.

VII. CONCLUSION

1) This paper proposes a delay dependent sliding mode variable structure control, based on LMI, to suppress the vibration of the MRD suspension system. In accordance with the nonlinear characteristics of MRD, a dynamic model of automotive semi-active suspension, considering time delay, is established. By defining a parameter-dependent Lyapunov switching functional, the conditions for asymptotic stability of closed-loop time delay system are derived, while the sliding mode variable structure control of reduced conservatism is designed. According to the method of LMI, the asymptotic stability problem of sliding mode is transformed into a feasibility problem, which can be solved by the solver 'feasp' in LMI toolbox. In addition, the calculation of the

critical time delay of semi-active suspension system is also expressed as a generalized eigenvalue optimization problem.

2) The prototype of MRD is produced on trial basis, while the time delay measurement of MRD is carried out on a material testing machine. According to the test results, the time delay of the designed MRD is no more than 28ms and it offers high dynamic response speed. The critical time delay of MRSS is calculated at 32.4ms, through the optimization problem. When the time delay is greater than the critical time delay, the stability of the sliding mode cannot be guaranteed, resulting in the instability of the MRSS system.

3) The simulation and real vehicle test have validated that, the MRSS performance is improved, when using the designed delay dependent sliding mode variable structure controller, despite the actuator time delay. However, this work only studies the time delay dependent sliding mode controller for a quarter of a vehicle. Nonetheless, the body attitudes, such as roll and pitch control, need also to be further studied. The implementation of new design techniques for MRSS system would be an interesting topic of future research.

REFERENCES

[1] X. Ma, P. K. Wong, and J. Zhao, "Practical multi-objective control for automotive semi-active suspension system with nonlinear hydraulic adjustable damper," *Mech. Syst. Signal Process.*, vol. 117, pp. 667–688, Feb. 2019, doi: 10.1016/j.ymssp.2018.08.022.

[2] M. Saad, S. Akhtar, A. K. Rathore, Q. Begume, and M. Reyaz-ur-Rahim, "Control of semi-active suspension system using PID control," *IOP Conf. Ser. Mater. Sci. Eng.*, vol. 404, no. 1, pp. 12–39, 2018, doi: 10.1088/1757-899X/404/1/012039.

[3] H. Zhu, J. Yang, and Y. Zhang, "Nonlinear dynamic model of air spring with a damper for vehicle ride comfort," *Nonlinear Dyn.*, vol. 89, no. 4, pp. 1–24, 2017, doi: 10.1007/s11071-017-3535-9.

[4] B. Tang and M. J. Brennan, "A comparison of two nonlinear damping mechanisms in a vibration isolator," *J. Sound Vib.*, vol. 332, no. 3, pp. 225–239, 2013, doi: 10.1016/j.jsv.2012.09.010.

[5] U. Solomon and C. Padmanabhan, "Semi-active hydro-gas suspension system for a tracked vehicle," *J. Terramech.*, vol. 48, no. 3, pp. 510–520, 2011, doi: 10.1016/j.jterra.2011.01.002.

[6] J. H. Park, W. H. Kin, and C. S. Shin, "A comparative work on vibration control of a quarter car suspension system with two different Magneto-rheological damper," *Smart Mater. Struct.*, vol. 27, no. 1, pp. 1–10, 2017, doi: 10.1088/1361-665X/26/1/015009.

[7] R. Jeyasenthil, D. Yoon, S. Choi, and G. Kim, "Robust semiactive control of a half-car vehicle suspension system with magnetorheological dampers: Quantitative feedback theory approach with dynamic decoupler," *Int. J. Robust Nonlinear Control*, vol. 31, no. 4, pp. 1418–1435, Mar. 2021, doi: 10.1002/rnc.5355.

[8] H. L. Zhang, E. Wang, and N. Zhang, "Semi-active sliding mode control of vehicle suspension with magneto-rheological damper," *Chin. J. Mech. Eng.*, vol. 28, no. 1, pp. 1–13, 2015, doi: 10.3901/CJME.2014.0918.152.

[9] W. J. Wang, Y. Liang, and E. Wang, "Comparison on models of controllable magneto-rheological dampers," *Chin. J. Mech. Eng.*, vol. 45, no. 9, pp. 100–108, 2009, doi: 10.3901/JME.2009.09.100.

[10] M. S. Mian, E. N. Chatzi, and V. K. Dertimanis, "Nonlinear modeling of a rotational MR damper via an enhanced Bouc-Wen model," *Smart Mater. Struct.*, vol. 24, no. 10, pp. 105–120, 2015, doi: 10.1088/0964-1726/24/10/105020.

[11] H. Yu, X. Sun, and J. Xu, "The time-delay coupling nonlinear effect in shy-hook control of vibration isolation systems using magneto-rheological fluid dampers," *J. Mech. Sci. Technol.*, vol. 30, no. 9, pp. 4157–4166, 2016, doi: 10.1007/s12206-16.-0827-9.

[12] H. L. Zhang, E. Wang, and F. H. Min, "Skyhook-based semi-active control of full-vehicle suspension with magneto-rheological dampers," *Chin. J. Mech. Eng.*, vol. 26, no. 3, pp. 511–518, 2013, doi: 10.3901/CJME.2013.03.498.

[13] H. D. Choi, C. K. Ahn, M. T. Lim, and M. K. Song, "Dynamic output-feedback H_∞ control for active half-vehicle suspension systems with time-varying input delay," *Int. J. Control, Autom. Syst.*, vol. 14, no. 1, pp. 59–68, Feb. 2016, doi: 10.1007/s12555-015-2005-8.

[14] C. Hua, J. Chen, Y. Li, and L. Li, "Adaptive prescribed performance control of half-car active suspension system with unknown dead-zone input," *Mech. Syst. Signal Process.*, vol. 111, pp. 135–148, Oct. 2018, doi: 10.1016/j.ymssp.2018.03.048.

[15] J. Mrazgua, E. H. Tisssir, and M. Ouahi, "Fuzzy fault-tolerant H_∞ control approach for nonlinear active suspension systems with actuator failure," *Proc. Comput. Sci.*, vol. 148, pp. 465–474, Jan. 2019, doi: 10.1016/j.procs.2019.01.059.

[16] L. Ming, L. Yibin, R. Xuewen, Z. Shuaishuai, and Y. Yanfang, "Semi-active suspension control based on deep reinforcement learning," *IEEE Access*, vol. 8, pp. 9978–9986, 2020, doi: 10.1109/ACCESS.2020.2964116.

[17] B. Vanavil and K. K. Chaitanya, "Improved PID control design for unstable time delay processes based on direct synthesis method and maximum sensitivity," *Int. J. Syst. Sci.*, vol. 46, no. 8, pp. 1349–1366, 2015, doi: 10.1080/00207721.2013.822124.

[18] C. C. Chen and S. C. Chang, "Stability, bifurcation and chaos of nonlinear active suspension system with time-delay feedback control," *J. Adv. Transp.*, vol. 2018, pp. 1–12, Jan. 2018, doi: 10.1155./2018/4218175.

[19] H. Y. Hu and Z. H. Wang, "Nonlinear dynamics of controlled mechanical systems with time delays," *Prog. Natural Sci.*, vol. 10, no. 11, pp. 801–811, 2000, doi: 10.1007/978-3-662-05030-9-8.

[20] M. Hosek, N. Olgac, and H. Elmali, "The centrifugal delayed resonator as a tunable torsional vibration absorber for multi degree of freedom systems," *J. Vibrat. Control*, vol. 5, no. 2, pp. 299–332, 1999, doi: 10.1177/107754639900500209.

[21] N. Jalili and N. Olgac, "A sensitivity study on optimum delayed feedback vibration absorber," *J. Dyn. Syst., Meas., Control*, vol. 122, no. 2, pp. 314–321, Jun. 2000, doi: 10.1115/1.482457.

[22] S. Bououden, M. Chadli, L. Zhang, and T. Yang, "Constrained model predictive control for time-varying delay systems: Application to an active car suspension," *Int. J. Control, Autom. Syst.*, vol. 14, no. 1, pp. 51–58, Feb. 2016, doi: 10.1007/s12555-015-2009-4.

[23] B. Zhou, "Input delay compensation of linear systems with both state and input delays by nested prediction," *Automatica*, vol. 50, no. 5, pp. 1434–1443, May 2014, doi: 10.1016/j.automatica.2014.03.010.

[24] P. L. Li and M. X. Fang, "Time-delay H_∞ control for active suspension system of wheel driven electric vehicles," *Noise Vibrat. Control*, vol. 40, no. 4, pp. 137–141, 2020, doi: 10.3969/j.issn.1006-1355.2020.04.025.

[25] S.-Y. Han, C.-H. Zhang, and G.-Y. Tang, "Approximation optimal vibration for networked nonlinear vehicle active suspension with actuator time delay," *Asian J. Control*, vol. 19, no. 3, pp. 983–995, May 2017, doi: 10.1002/asjc.1419.

[26] H. Du, N. Zhang, and J. Lam, "Parameter-dependent input-delayed control of uncertain vehicle suspensions," *J. Sound Vibrat.*, vol. 317, nos. 3–5, pp. 537–556, Nov. 2008, doi: 10.1016/j.jsv.2008.03.066.

[27] H. Li, X. Jing, and H. R. Karimi, "Output-feedback-based H_∞ control for vehicle suspension systems with control delay," *IEEE Trans. Ind. Electron.*, vol. 61, no. 1, pp. 436–446, Jan. 2014, doi: 10.1109/TIE.2013.2242418.

[28] M. Yokoyama, J. K. Hedrick, and S. Toyama, "A model following sliding mode controller for semi-active suspension systems with MR dampers," in *Proc. Amer. Control Conf.*, Jun. 2001, pp. 2652–2657, doi: 10.1109/acc.2001.946276.

[29] H. Pan, W. Sun, H. Gao, and X. Jing, "Disturbance observer-based adaptive tracking control with actuator saturation and its application," *IEEE Trans. Autom. Sci. Eng.*, vol. 13, no. 2, pp. 868–875, Apr. 2016, doi: 10.1109/TASE.2015.2414652.

[30] V. S. Deshpande and P. D. Shendge, "Active suspension systems for vehicles based on a sliding mode controller in combination with inertial delay control," *Proc. Inst. Mech. Eng. D J. Automobile Eng.*, vol. 227, no. 5, pp. 675–690, 2013, doi: 10.1177/095447012462953.

[31] T. H. Wang and X. M. Zhao, "Intelligent second-order sliding mode control based on recurrent radial basis function neural network for permanent magnet linear synchronous motor," *Trans. China Electrotech. Soc.*, vol. 36, no. 6, pp. 1229–1237, 2021, doi: 10.19595/j.cnki.1000-6753.tces.191238.

[32] M. Xu, Q. S. Huang, and G. Li, "Switch-optimal control of vehicle magneto -rheological semi-active suspension," *Noise Vibrat. Control*, vol. 40, no. 6, pp. 159–164, 2020, doi: 10.06-1355(2020)06-0159-06.

[33] J.-H. Koo, F. D. Goncalves, and M. Ahmadian, "A comprehensive analysis of the response time of MR dampers," *Smart Mater. Struct.*, vol. 15, no. 2, pp. 351–358, Apr. 2006, doi: 10.1088/0964-1726/15/2/015.

[34] H. Li, X. Jing, and H. R. Karimi, "Output-feedback-based H_∞ control for vehicle suspension systems with control delay," *IEEE Trans. Ind. Electron.*, vol. 61, no. 1, pp. 436–446, Jan. 2014, doi: 10.1109/TIE.2013.2242418.

MAOFEI ZHU was born in Hefei, Anhui, China, in 1983. He received the Ph.D. degree in automotive engineering from the School of Automotive and Traffic Engineering, Hefei University of Technology, Hefei, in 2011.

He is currently an Assistant Professor with the School of Advanced Manufacturing Engineering, Hefei University, Hefei. He has authored or coauthored over 15 articles and holds 20 patents. His research interests include vehicle system dynamics and control, intelligent vehicle control by wire, and advanced driver assistance systems.

GANG LV was born in Laian, Anhui, China, in 1978. He is currently a Professor with the School of Advanced Manufacturing Engineering, Hefei University, Hefei, China. He has authored or coauthored over 30 articles and holds ten patents. His research interests include image processing technology, intelligent driving vehicle perception technology, and target detection and tracking technology based on deep learning.

CHUNPENG ZHANG was born in Xuzhou, Jiangsu, China, in 1980. He received the master's degree in automotive engineering from the School of Automotive and Traffic Engineering, Hefei University of Technology, Hefei, China, in 2007.

He is a Senior Experimentalist with the School of Advanced Manufacturing Engineering, Hefei University, Hefei. He has authored or coauthored over ten articles and holds five patents. His research interests include mechanical dynamics, mechanical structure design, robot control system design.

JIANMAN JIANG was born in Suzhou, Anhui, China, in 1986. She received the Ph.D. degree in automotive engineering from the School of Automotive and Traffic Engineering, Hefei University of Technology, Hefei, China, in 2017.

She is currently a Senior Engineer with the Technical Center, Anhui Jianghuai Automobile Company Ltd., Hefei. Her research interests include simulation and verification of autonomous vehicle and safety of the intended functionality of autonomous vehicle.

HUIRAN WANG was born in Chaohu, Anhui, China, in 1991. He received the Ph.D. degree in automotive engineering from the School of Automotive and Traffic Engineering, Hefei University of Technology, Hefei, China, in 2021.

He is currently a Lecturer with the School of Advanced Manufacturing Engineering, Hefei University, Hefei. His research interests include automotive system dynamics and control and active safety control system design.